

Structure–Activity Relationships of Acetylcholinesterase Noncovalent Inhibitors Based on a Polyamine Backbone. 2. Role of the Substituents on the Phenyl Ring and Nitrogen Atoms of Caproctamine

Vincenzo Tumiatti,[†] Michela Rosini,[†] Manuela Bartolini,[†] Andrea Cavalli,[†] Gabriella Marucci,[‡] Vincenza Andrisano,[†] Piero Angeli,[‡] Rita Banzi,[†] Anna Minarini,[†] Maurizio Recanatini,[†] and Carlo Melchiorre^{*†}

Department of Pharmaceutical Sciences, University of Bologna, Via Belmeloro 6, 40126 Bologna, Italy, and Department of Chemical Sciences, University of Camerino, Via S. Agostino 1, 62032 Camerino (MC), Italy

Received October 2, 2002

Continuing our studies on polyamine-based compounds of potential interest in the field of Alzheimer's disease therapeutics, we investigated the structure–activity relationships (SAR) of a lead compound (caproctamine, **3**) identified in a previous work. In particular, we varied the substituents on the phenyl ring and on the nitrogen functions (both the amine and the amide), and studied the effects of such modifications on the inhibitory potency against isolated acetyl- and butyryl-cholinesterase (AChE and BChE). Moreover, the ability of selected compounds to reverse the D-tubocurarine-induced neuromuscular blockade and their antagonism toward muscarinic M₂ receptors in guinea pig left atrium were assayed. The most interesting SAR result was the identification of a relationship between the electronic characteristics of 2-substituents (measured by p*K_a*) and the AChE inhibitory potency (pIC₅₀) of tertiary amine compounds **6–12**, which was confirmed by the invariance of the pIC₅₀ values of the corresponding methiodide derivatives **14–20**. With regard to the biological profile, the most interesting compound was the *N*-ethyl-analogue of caproctamine (**9**), that showed pIC₅₀ values of 7.73 (±0.02) and 5.65 (±0.03) against AChE and BChE, respectively. The ability to increase the acetylcholine level was maintained in the functional assay (pAI₅₀ for reversing the neuromuscular blockade was 6.45 (±0.07)), as well as the ability to antagonize the M₂ receptors (p*K_b* = 5.65 (±0.06)). Moreover, **9** showed a long duration of action as AChE inhibitor, an useful property in view of a possible development of this compound as a therapeutic agent.

Introduction

Inhibitors of acetylcholinesterase (AChE) are important in controlling diseases that involve impaired acetylcholine-mediated neurotransmission, including Alzheimer's disease (AD), the most common cause of dementia in elderly patients, which involves selective loss of cholinergic neurons in the brain.^{1–3} To date, the cholinergic hypothesis is still the most successful approach in alleviating the symptoms of AD. However, despite an enormous amount of work, only few inhibitors of AChE, such as tacrine, donepezil, rivastigmine, and galantamine (Figure 1), have been approved for the symptomatic treatment of AD and they do not even address the etiology of the disease for which are used.^{4–8} Recent efforts have led to the development of additional AChE inhibitors whose efficacy is under clinical evaluation.⁷

AChE is the enzyme involved in the hydrolysis of the neurotransmitter acetylcholine (ACh) at cholinergic synapses in the central and peripheral nervous system. Inhibitors of AChE activity promote an increase in the concentration and the duration of action of synaptic ACh thus causing an enhancement of the cholinergic trans-

mission through the activation of the synaptic nicotinic and muscarinic receptors. It has been demonstrated that AChE could play a key role during an early step in the development of the senile plaques, as revealed by the finding that AChE accelerates β -amyloid peptide ($A\beta$) deposition.⁹ Active site inhibitors, such as edrophonium, did not affect this peculiar feature of AChE, which was affected by peripheral binding site ligands, such as decamethonium and propidium. Interestingly enough, butyrylcholinesterase (BChE), an enzyme that lacks the peripheral binding site, did not affect amyloid formation. This finding suggests clearly that the catalytic site of AChE does not participate in the interaction of the enzyme with $A\beta$, whereas it is possible that the peripheral binding site of AChE may be involved in amyloid formation.⁹

Consequently, the design of ligands able to interact simultaneously with catalytic and peripheral sites should implicate advantages over the known AChE inhibitors. Clearly, inhibition of the peripheral binding site would prevent the aggregation of $A\beta$ induced by AChE. Following this reasoning, our group has started a research project aimed at producing novel ligands based on a polyamine backbone, having affinity for both AChE active and peripheral binding sites and for muscarinic M₂ receptors as well. It was advanced that drugs able to antagonize selectively presynaptic muscarinic M₂ autoreceptors may also be useful in AD as they would facilitate ACh release in the synapse.¹⁰

* Corresponding author: Carlo Melchiorre, Department of Pharmaceutical Sciences, University of Bologna, Via Belmeloro 6, 40126 Bologna, Italy. Tel. +39-051-2099706. Fax: +39-051-2099734. E-mail: camelch@kaiser.alma.unibo.it.

[†] University of Bologna.

[‡] University of Camerino.

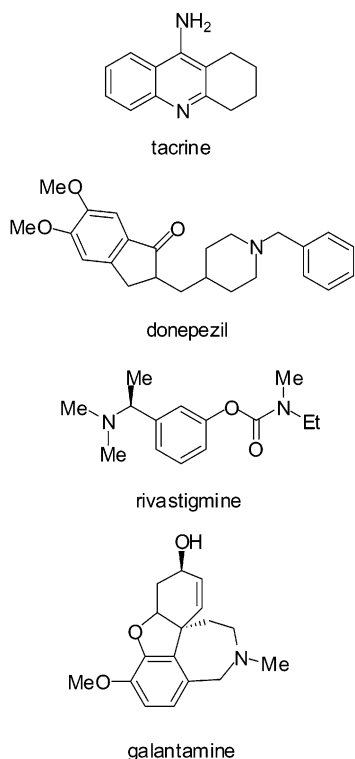


Figure 1. Chemical structure of AChE inhibitors in current use for the treatment of Alzheimer's disease.

The starting point of our study was the observation that benextramine (**1**, Figure 2), the prototype of tetraamine disulfides for irreversible inhibition of α -adrenoceptors,¹¹ displayed also a significant affinity for cardiac muscarinic M_2 receptors and potentiated the effect of ACh on the frog rectus.^{12,13} Subsequently, the finding that **1** was a reversible inhibitor of AChE has provided the opportunity to apply the universal template approach to the design of polyamines displaying affinity for AChE and muscarinic M_2 receptors.¹⁰

In a preliminary study, we have shown that the disulfide bridge of **1** is not required for AChE inhibition because the corresponding carbon analogue was as

active as the prototype. Furthermore, we have established that optimum inhibition of AChE activity is dependent on the carbon chain separating the inner nitrogen atoms of carbon analogues of **1**. Although optimum inhibition of AChE was observed for the tetraamine bearing a heptamethylene spacer between the inner nitrogen atoms, we have chosen as lead compound the higher homologue tetraamine methoctramine (**2**, Figure 2), carrying eight methylenes, because it displayed optimum affinity for muscarinic M_2 receptors.¹⁰ Taking into account the observation that a diamine diamide backbone retained significant affinity for muscarinic M_2 receptors, the structure of **2** was modified by replacing the two inner amine functions with amide groups such as to improve the overall lipophilicity, which might be important for penetrating the brain. This study led to the discovery of caproctamine (**3**, Figure 2), which became our new lead. It emerged as a powerful tool for investigating the neurological disorders due to a loss in the cholinergic system. In comparison with **1**, **3** was 42-fold more potent at AChE, while being 2-fold less potent at BChE with a AChE/BChE selectivity ratio of 68. Furthermore, it was a weak antagonist at both muscarinic M_1 and M_3 receptors, while displaying an affinity toward muscarinic M_2 receptors similar to the affinity for AChE as revealed by a comparison of pA_2 (M_2) and pIC_{50} (AChE) values which were 6.39 and 6.77, respectively. It was also established that **3** caused a mixed type of inhibition, that is, inhibition of both the active site and a second distal site of the enzyme.¹⁰

The present article expands on the study of another aspect of structure–activity relationships of prototype **3**, namely, the effect of substituents on the phenyl ring and of *N*-alkyl substituents on the four nitrogen atoms. The presence of a 2-methoxybenzyl group seems to play a crucial role for the affinity toward AChE as revealed by the unsubstituted analogue of **1**, which inhibited AChE only at millimolar concentration. This finding offers the opportunity to examine the effect of different aromatic substituent parameters such as Hammett σ and Hansch π values on both affinity and selectivity for

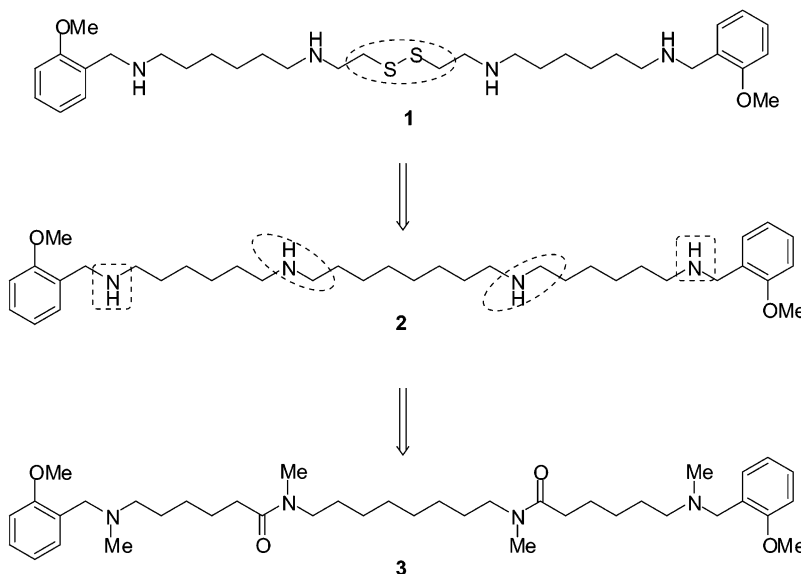
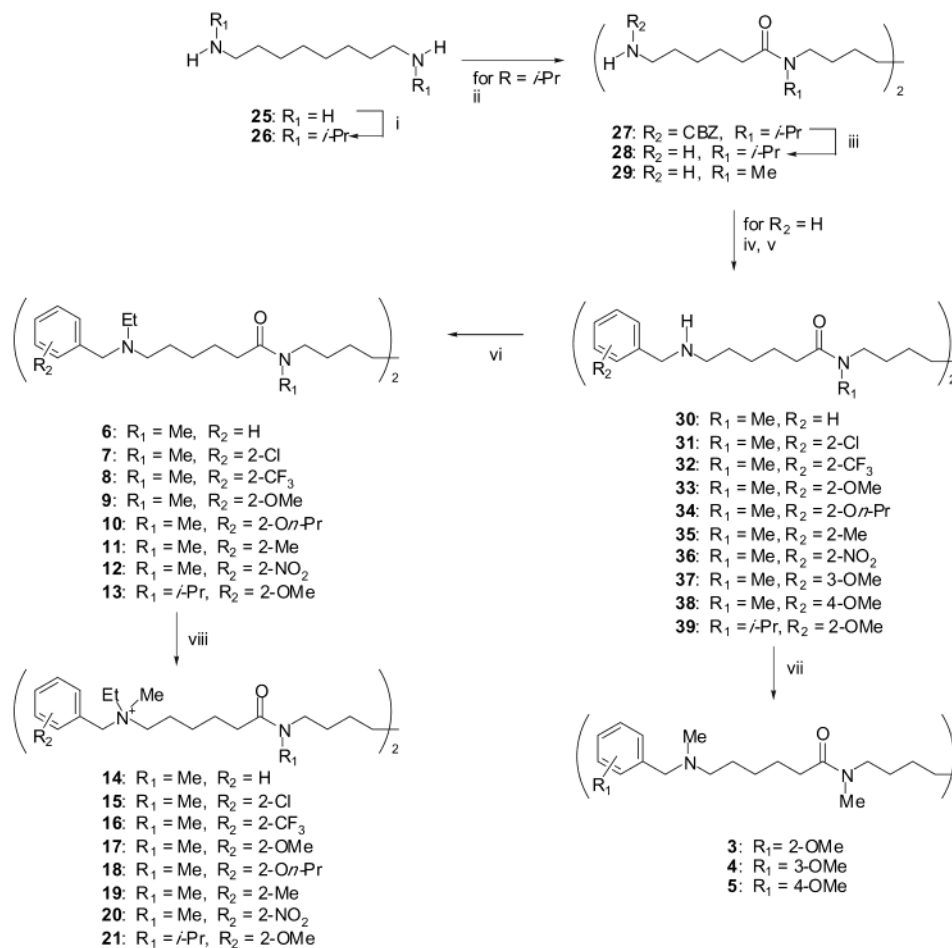


Figure 2. Chemical structure of benextramine (**1**), methoctramine (**2**), and caproctamine (**3**). The design strategy for the development of **3** is also shown.

Scheme 1^a

^a CBZ, $\text{C}_6\text{H}_5\text{CH}_2\text{OCO}-$; i, NaBH_4 , MeCOMe ; ii, $\text{CBZ-NH}(\text{CH}_2)_5\text{COOH}$, Et_3N , EtOCOCl , dioxane; iii, HBr , CH_3COOH ; iv, $\text{R}_2\text{-C}_6\text{H}_4\text{CHO}$, toluene; v, NaBH_4 , EtOH ; vi, $(\text{EtO})_2\text{SO}_2$; vii, HCOOH , HCHO ; viii, MeI , MeCOMe .

AChE over BChE. It is known that for relevant quantitative structure–activity relationships at least 12 carefully selected compounds are necessary to obtain a significant two-parameter equation. In the present study, our aim was to determine only whether electronic and/or lipophilic properties of aromatic substituents of **3**-related compounds could exert any favorable effect on AChE selectivity and affinity rather than assess a quantitative relationship. It seemed this could be determined with a few properly chosen substituents. These were selected to have σ and π values in a positive or negative direction, in all combinations. Comparison of the AChE inhibition of these substituted derivatives with the unsubstituted analogue **6** should reveal the importance, if any, of one or both these parameters. The compounds used were the chloro and trifluoromethyl ($+\pi$, $+\sigma$) (**7** and **8**), methoxy ($-\pi$, $-\sigma$) (**9**), *n*-propoxy and methyl ($+\pi$, $-\sigma$) (**10** and **11**), and nitro ($-\pi$, $+\sigma$) (**12**) derivatives. To verify whether the aromatic substituent at position 2 might have any influence on the basicity and, as a consequence, on the extent of protonation of the outer nitrogen atom, we synthesized also the corresponding methiodides **14–21** of **6–13**, which bear a permanent positive charge.

Since the presence of a 2-methoxy function, as in **9**, conferred optimum affinity for AChE, we investigated also analogues **4** and **5** in which the 2-methoxy group was moved at positions 3 and 4, respectively. In this

case, the choice of **3** as lead compound was dictated by the fact that the synthesis of *N*-methyl derivatives was easier than that of the corresponding *N*-ethyl analogues.

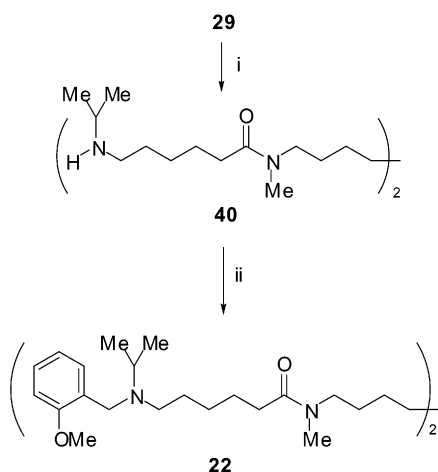
Next, to verify the effect of the *N*-alkylation of nitrogen atoms of the tetraamine backbone we replaced the hydrogen atom of **33** with a methyl, ethyl, and *i*-propyl group, affording **3**, **9**, and **22**, respectively. Similarly, we replaced the *N*-methyl group of **9** with an *N*-*i*-propyl group, affording **13**. Notwithstanding several efforts, we were not able to synthesize the *N*-ethyl homologue of **9**.

Finally, to investigate on the role of amide functions of **9** in the interaction with AChE, we included in the present study compound **23** and its methiodide analogue **24**.

Chemistry

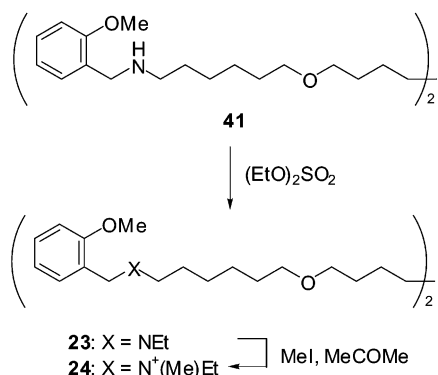
All the compounds were synthesized by standard procedures (Schemes 1–3) and were characterized by IR, ^1H NMR, mass spectra, and elemental analysis.

Compound **29**¹⁴ was the starting material for the synthesis of compounds **6–12**, **14–20**, and **22**. Alkylation of the commercially available diamine **25** with acetone via Schiff base in the presence of NaBH_4 afforded **26**, which was reacted with *N*-[(benzyloxy)carbonyl]-6-aminocaproic acid to give **27**. Removal of the *N*-(benzyloxy)carbonyl group of **27** by hydrolysis with HBr gave diamine diamide **28**.

Scheme 2^a

^a i, H₂/Pd, MeCOMe; ii, 2-MeO-C₆H₄-CH₂Cl, DMF.

Scheme 3



Diamine diamides **28** and **29**¹⁴ were treated with the appropriate substituted benzaldehyde followed by reduction with NaBH₄ of the formed Schiff base to the corresponding dibenzyl derivatives **30–39** (Scheme 1). Diethylation of **30–39** to afford **6–13** was performed by using diethylsulfate in toluene at refluxing temperature (Scheme 1). The state of the reaction was continuously monitored to avoid possible quaternization of amine functions. Similarly, **41**¹⁵ was treated with diethylsulfate to give **23** (Scheme 3). Methiodides **14–21** and **24** were prepared by methylation of the corresponding tertiary diamine with an excess of methyl iodide (Schemes 1 and 3).

3-Methoxy and 4-methoxy **4** and **5** derivatives were synthesized by Eschweiler–Clarke methylation of compounds **37** and **38**, respectively (Scheme 1).

Compound **22** was synthesized using a different synthetic pathway as shown in Scheme 2. Thus, dialkylation of **29** was performed by alkylation with acetone in reducing conditions, using catalytic hydrogenation over 10% palladium on charcoal, to give **40**. Finally, compound **40** was treated with 2-methoxybenzyl chloride to afford derivative **22**.

An inspection of ¹H NMR data reveals that different rotamers around the amide C–N bond are present in solution. In fact, all the signals relative to N–CH₃ protons are split into two singlets. For instance, in compound **9** (and many others, see Experimental Section), the signals at δ 2.90 ppm (s, 3H) and 2.96 ppm (s, 3H) correspond to different rotamers of the amide N–CH₃ groups. Under freely rotating conditions around

the amide C–N bond, a unique singlet should be observed. The presence of rotamers (*E/E*, *E/Z*, and *Z/Z*) complicated also ¹³C NMR spectra. In compound **9**, the two amide N–CH₃ groups were split into three signals at δ 33.88, 33.60, and 33.27 ppm, respectively.

Biology

To determine the potential interest of compounds **4–24** for the treatment of AD, their AChE inhibitory activity was determined by the method of Ellman et al.¹⁶ on AChE from human erythrocytes. Furthermore, to establish the selectivity of **4–24**, their BChE inhibitory activity was also calculated by the same method on BChE from human serum. The inhibitory potency was expressed as pIC₅₀ values, which represent the minus logarithm of the concentration of inhibitor required to decrease enzyme activity by 50%. To allow comparison of the results, **1–3**, tacrine, and physostigmine were used as the reference compounds.

Selected compounds were further analyzed in a peripheral cholinergic synapse, such as skeletal neuromuscular junction, by determining the ability to reverse the D-tubocurarine-induced neuromuscular blockade, which is a well-known effect of AChE inhibitors. The results were expressed as pAI₅₀ values, which represent the minus logarithm of the concentration of inhibitor that reaches 50% of antagonism index (AI).^{17,18} Tacrine, physostigmine, and **3** were used as the reference compounds.

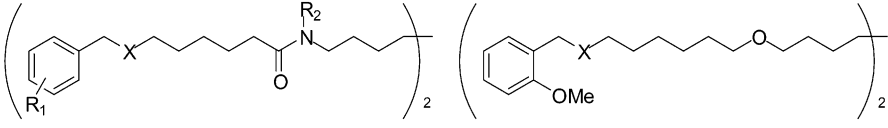
The mechanism of the AChE inhibition was deeply studied for one representative compound (**9**) of the series, using prototype **3** as the reference compound.

Functional activity at muscarinic receptors was determined by the use of the muscarinic M₂ receptor-mediated negative inotropism in driven guinea pig left atria (1 Hz). This method has been described in detail earlier.¹⁹ The biological results were expressed as pK_b values determined according to van Rossum.²⁰

Results and Discussion

The inhibitory potency, expressed as pIC₅₀ values, of compounds **4–24** of AChE and BChE from human erythrocytes and human serum, respectively, is reported in Table 1 in comparison with that of prototype polyamines benextramine (**1**), methoctramine (**2**), and caproctamine (**3**), and well-known AChE inhibitors such as tacrine and physostigmine. Furthermore, **6–12** and **17** were evaluated also for their ability to reverse the skeletal neuromuscular junction blockade in rat phrenic nerve-hemidiaphragm in comparison with **3**, tacrine, and physostigmine. In addition, the antagonism at muscarinic M₂ receptors was determined for compounds **7–9**.

Recently, we reported that **3** was endowed with a well-balanced affinity profile as an AChE inhibitor and a competitive muscarinic M₂ receptor antagonist.¹⁰ Furthermore, it was shown that **3** was able to bind at both the catalytic and the peripheral sites of AChE. Consequently, **3** emerged as a valuable tool in investigating AD because, besides its effects on the cholinergic system, it might also prevent AChE-mediated A β aggregation by interacting with the peripheral anionic binding site of AChE. These promising results prompted us to perform structural modifications on the structure of **3**

Table 1. Inhibition of AChE and BChE Activities by Polyamines


no. ^a	R ₁	X	R ₂	pIC ₅₀ ^b		AChE/BChE ^c	pAI ₅₀ ^d	pK _a ^e	pK _b (M ₂) ^f
				AChE	BChE				
1 ^g				5.14 ± 0.02	5.21 ± 0.03	0.9	nd ^h	nd	nd
2 ^g				5.27 ± 0.03	6.01 ± 0.02	0.2	nd	nd	7.92 ± 0.08 ⁱ
3	2-OMe	NMe	Me	6.77 ± 0.01	4.93 ± 0.04	68	5.79 ± 0.07	nd	6.39 ± 0.23 ⁱ
4	3-OMe	NMe	Me	6.17 ± 0.04	5.08 ± 0.03	12	nd	nd	nd
5	4-OMe	NMe	Me	5.24 ± 0.02	5.26 ± 0.03	1	nd	nd	nd
6	H	NEt	Me	7.31 ± 0.03	5.97 ± 0.02	21	6.32 ± 0.13	7.42 ± 0.04	nd
7	2-Cl	NEt	Me	6.95 ± 0.15	5.39 ± 0.04	37	7.19 ± 0.04	6.92 ± 0.04	5.61 ± 0.31
8	2-CF ₃	NEt	Me	5.34 ± 0.04	3.78 ± 0.08	36	6.84 ± 0.02	6.15 ± 0.04	<5
9	2-OMe	NEt	Me	7.73 ± 0.02	5.65 ± 0.03	121	6.45 ± 0.07	7.80 ± 0.06	5.65 ± 0.6
10	2- <i>o</i> nPr	NEt	Me	7.47 ± 0.03	6.78 ± 0.02	5	6.19 ± 0.02	7.75 ± 0.05	nd
11	2-Me	NEt	Me	7.25 ± 0.05	5.13 ± 0.03	132	6.35 ± 0.01	7.46 ± 0.02	nd
12	2-NO ₂	NEt	Me	6.10 ± 0.03	4.26 ± 0.08	69	5.93 ± 0.02	6.26 ± 0.03	nd
13	2-OMe	NEt	<i>i</i> Pr	7.74 ± 0.04	5.67 ± 0.04	118	nd	nd	nd
14	H	N ⁺ (Me)Et	Me	7.43 ± 0.02	5.60 ± 0.03	69	nd	nd	nd
15	2-Cl	N ⁺ (Me)Et	Me	7.71 ± 0.02	5.59 ± 0.02	133	nd	nd	nd
16	2-CF ₃	N ⁺ (Me)Et	Me	7.93 ± 0.13	5.12 ± 0.03	640	nd	nd	nd
17	2-OMe	N ⁺ (Me)Et	Me	7.92 ± 0.02	5.85 ± 0.01	118	7.21 ± 0.02	nd	nd
18	2- <i>o</i> nPr	N ⁺ (Me)Et	Me	7.76 ± 0.03	7.08 ± 0.04	5	nd	nd	nd
19	2-Me	N ⁺ (Me)Et	Me	7.78 ± 0.05	5.19 ± 0.05	388	nd	nd	nd
20	2-NO ₂	N ⁺ (Me)Et	Me	7.91 ± 0.06	5.62 ± 0.02	196	nd	nd	nd
21	2-OMe	N ⁺ (Me)Et	<i>i</i> Pr	8.09 ± 0.02	5.78 ± 0.04	204	nd	nd	nd
22	2-OMe	N <i>i</i> Pr	Me	7.14 ± 0.13	6.06 ± 0.03	12	nd	nd	nd
23		NEt		6.69 ± 0.06	5.58 ± 0.02	13	nd	nd	nd
24		N ⁺ (Me)Et		7.11 ± 0.02	6.12 ± 0.03	10	nd	nd	nd
tacrine				6.60 ± 0.02	7.27 ± 0.02	0.2	6.33 ± 0.03	nd	nd
physostigmine				7.75 ± 0.18	7.64 ± 0.15	1	6.50 ± 0.04	nd	nd

^a **1**, **2**, tetrahydrochlorides; **3–13**, **23**, dioxalates; **14–21**, **24**, diiodides. ^b AChE and BChE were from human erythrocytes and human serum, respectively. pIC₅₀ values represent the negative logarithm of the concentration of inhibitor required to decrease enzyme activity by 50% and are the mean of two independent measurements, each performed in triplicate. ^c The AChE/BChE selectivity ratio is the antilog of the difference between pIC₅₀ values at AChE and BChE, respectively. ^d pAI₅₀ values represent the negative logarithm of inhibitor concentration that reaches 50% of antagonism index (AI), i.e., the ability to reverse the D-tubocurarine-induced neuromuscular blockade.¹⁷ ^e Apparent dissociation constants taken from ref 19. ^f pK_b values (± SE, *n* = 4) were calculated according to Van Rossum²⁰ at 10 μM concentration at muscarinic M₂ receptors in guinea pig left atrium. ^g See Figure 2 for structure. ^h nd, not determined. ⁱ Data from ref 10.

to improve its biological profile. An examination of the results in Table 1 shows how AChE inhibitory activity can be affected markedly by an appropriate substituent on the nitrogen atoms and on the phenyl ring.

Our study began with an evaluation of AChE and BChE inhibitory activity due to the substituent on the outer and inner nitrogen atoms of the polyamine backbone of **3**. We had already shown that *N*-methylation of the corresponding analogue of **3**, bearing secondary amine and amide functions, resulted in a significant increase (~10-fold) in AChE inhibitory activity, while not affecting BChE inhibitory activity.¹⁰ In the present investigation, we replaced the methyl group of amine functions of **3** with ethyl and *i*-propyl groups, affording **9** and **22**, respectively. The *N*-ethyl analogue **9** was more potent than both *N*-methyl (**3**) and *N*-*i*-propyl (**22**) derivatives as revealed by their pIC₅₀ values at AChE of 7.73 ± 0.02, 6.77 ± 0.01, and 7.14 ± 0.13, respectively (Table 1). Then, the inner nitrogen atoms of **9** were modified by exchanging the methyl groups with *i*-propyl ones, affording **13**, which resulted as active as **9** at both AChE and BChE. It would be of interest to evaluate the corresponding *N*-ethyl analogue because it might help in identifying the substituent that would confer optimum AChE inhibitory activity. Unfortunately, we did not succeed in synthesizing the *N*-ethyl analogue of **9**.

To verify whether the 2-methoxy function of **9** (−*σ*,

−*σ*) has a role in the interaction with AChE and BChE, it was replaced by selected groups, affording analogues **6–8** and **10–12**, which have *π* and *σ* values in a positive or negative direction, in all combinations. An analysis of the results in Table 1 reveals that the 2-substituent has a role in the interaction with AChE. The 2-methoxy derivative **9** was the most potent of the series being 3- and 245-fold more potent than the unsubstituted analogue **6** and the 2-trifluoromethyl derivative **8**, respectively, which was the least potent of the series. The overall results obtained with these derivatives clearly indicate that lipophilic (*π*) or steric (expressed by molar refractivity, MR) characteristics of 2-substituents have little, if any, effect on AChE inhibitory activity in comparison with electronic properties (*σ*). It suffices to say that AChE inhibitory activity of **9** and **12**, albeit their *π* (−0.02 vs −0.28) and MR (7.87 vs 7.38) values are comparable, differed by a factor of 43. A possible interpretation of these results is that the substituents in **6–12** affect *N*-protonation through mixed inductive and mesomeric effects. This view was confirmed by the good correlation found for pIC₅₀ values and dissociation constants (pK_a)²¹ of basic AChE inhibitors **6–12** (Figure 3). If a most relevant effect of the 2-substituent of **6–12** on AChE inhibitory activity were to increase the basicity, then the pIC₅₀ value of an inhibitor having a permanent positive charge should not be dependent on

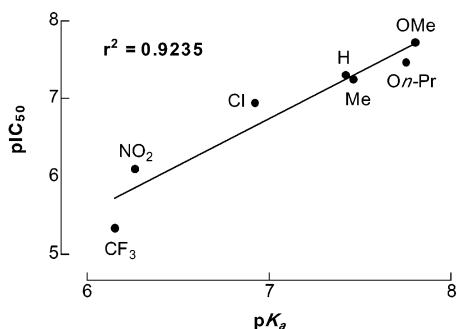


Figure 3. Relationship between AChE inhibiting activity (pIC_{50}) and the apparent dissociation constant (pK_a) of compounds **6**–**12**. The substituent at position 2 of the phenyl ring is indicated in the graph. The inset gives the squared correlation coefficient (r^2). Data from Table 1.

Table 2. Effect of pH on AChE Inhibitory Activity, Expressed as pIC_{50} Values, of **9** and **12** and of Their Corresponding Methiodides **17** and **20**

no.	pIC_{50}		
	pH = 7.0	pH = 7.5	pH = 8.0
9	7.79 ± 0.04	7.76 ± 0.05	7.73 ± 0.02
12	7.49 ± 0.06	7.10 ± 0.05	6.10 ± 0.03
17	7.96 ± 0.04	7.96 ± 0.06	7.92 ± 0.02
20	7.90 ± 0.05	7.89 ± 0.07	7.91 ± 0.06

the electronic properties of the substituent. To this end, we evaluated the corresponding methiodides **14**–**20** of **6**–**12**. It turned out that these compounds inhibited AChE activity with comparable pIC_{50} values comprised within a range of 0.5 log units, whereas pIC_{50} values for **6**–**12** differed by 2.4 log units. Clearly, the ortho-substituents of **14**–**20**, unlike those of the corresponding tertiary amino derivatives **6**–**12**, did not appear to play a role in the interaction with AChE.

To further support the hypothesis that the electronic properties affect the protonation of tertiary amino functions, we evaluated AChE inhibitory activity of compounds **9** and **12** in comparison with their corresponding methiodides **17** and **20** at different pH values, that is, 7.0, 7.5, and 8.0. The results reported in Table 2 show clearly that pIC_{50} values for the 2-methoxy derivative **9** and methiodides **17** and **20** were not affected by pH, whereas the pIC_{50} value of the 2-nitro derivative ($\sigma = 0.78$) was affected markedly by pH, confirming that the extent of protonation of the inhibitor has a significant effect on AChE inhibitory activity.

Since the 2-methoxy function was endowed with optimal electronic properties, we investigated also the effect on AChE inhibitory activity of moving the methoxy function from position 2 to positions 3 and 4, affording compounds **4** and **5**. It turned out that the affinity for AChE is dependent on the position of the methoxy function and follows the order 2-MeO > 3-MeO > 4-MeO, which is not in line with the observation that the pK_a was the most important parameter for AChE inhibitory activity, as one would expect the 4-MeO derivative **5** to be even more potent than **9**. However, this may be only an apparent contradiction because different effects (for instance, steric hindrance) other than the extent of protonation of the amine function might determine the lower potency of **5** relative to **9**.

Replacement of the amide function of **9** with a methylenoxy unit, affording **23**, resulted in a decrease

in AChE inhibitory activity. Similarly, the corresponding methiodide **24** of **23** was less potent than the corresponding methiodide **17** of **9**. Altogether, these results suggest clearly that the amide function of **9** cannot be exchanged for an ether moiety.

All of the compounds were significantly less potent in inhibiting BChE than AChE activity. The most potent compounds of the series in inhibiting BChE activity were the 2-*n*-propoxy derivatives **10** and **18**, whereas the least active were the 2-trifluoromethyl (**8**) and 2-nitro (**12**) derivatives. Most of the tertiary amino compounds were very selective for AChE, especially those having negative σ values such as **9**, **11**, and **13** by factors between 118 and 132. Since the AChE inhibitory activity of methiodides appeared to be not affected by the 2-substituent, the selectivity of methiodides bearing electron-withdrawing groups (positive σ values) for AChE was significantly increased in comparison with the corresponding tertiary amino derivatives.

Tertiary amino derivatives, which might have greater potential in AD over the corresponding methiodides, because of their lipophilicity, were assayed in rat nerve-hemidiaphragm preparation to determine their ability to reverse the neuromuscular blockade induced by D-tubocurarine. All of the tested compounds were more active than prototype **3**, and most of them were also more potent than tacrine (Table 1). The results in this assay did not parallel perfectly those obtained in determining AChE inhibitory activity. The most potent in reversing neuromuscular blockade were the 2-chloro (**7**) and 2-trifluoromethyl (**8**) derivatives with pIC_{50} values of 7.19 ± 0.04 and 6.84 ± 0.02 , respectively. The 2-methoxy derivative **9** was 19-fold less potent in reversing the neuromuscular blockade than in inhibiting AChE activity. The discrepancy between the results obtained in the two assays were observed also for AChE inhibitors with a different structure.²² It was argued that the determination of the AChE inhibition by biochemical studies determine the ability of a compound to inhibit enzyme activity, analyzing only the effect of a drug in a single mechanism. The pharmacological testing through the determination of neuromuscular blockade reversion analyzes the magnitude of an effect regardless of the implicated mechanisms. In other words, the pharmacological assay may give additional information relative to biochemical studies because it evaluates how the inhibitor enhances the activity of a cholinergic synapse and not merely the action on an isolated enzyme. Thus, it might be that a compound increases ACh release through mechanisms other than AChE inhibitory action.

To verify whether diamine diamides related to **3** possess affinity also for muscarinic M_2 receptors besides their AChE inhibition properties, compounds **7**–**9** were tested in the guinea pig left atrium. It turned out that **7** and **9** are weaker muscarinic M_2 receptor antagonists than prototype **3**, whereas the 2-trifluoromethyl derivative was devoid of affinity at $10 \mu\text{M}$ concentration (Table 1).

Clearly, the 2-methoxy derivative **9** was the most potent among tertiary amino derivatives in inhibiting AChE activity, being 9-fold more potent than prototype **3** with an AChE/BChE selectivity ratio of 121. Furthermore, **9** was more potent than tacrine and as active as

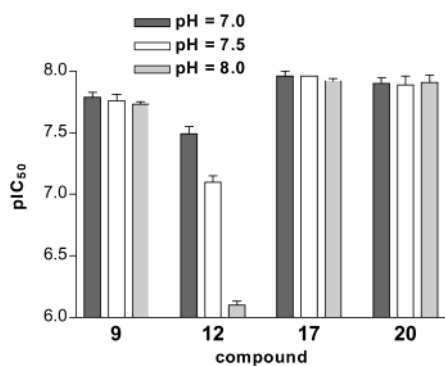


Figure 4. Effect of pH on the AChE inhibitory activity, expressed as pIC₅₀ values, of **9** and **12** in comparison with their corresponding methiodides analogues **17** and **20**.

physostigmine, which, contrary to **9**, inhibits AChE activity by way of covalent bond formation with the enzyme. In addition, **9** was more potent in reversing neuromuscular blockade at the skeletal junction than both **3** and tacrine, and was as active as physostigmine. Interestingly, **9** retained significant affinity also for muscarinic M₂ receptors, a property that may help in increasing ACh release in the synapse as a result of presynaptic muscarinic M₂ receptor blockade. Owing to this biological profile, **9** was studied further to characterize the nature of the AChE inhibitory activity.

Inhibition of AChE activity by **9** was very fast and not time-dependent, as 50% of enzyme inactivation produced by 18.6 nM concentration following 1-min incubation was not significantly different ($p > 0.01$) from the inhibition observed up to a 40-min incubation. The graphical analysis of steady-state inhibition data for **9** is shown in Figure 5, whereas the estimates of competitive inhibition constants K_i are reported in Table 3 in comparison with **3** and tacrine. It was found that **9**, like **3**, caused a mixed type of inhibition, that is, inhibition of both the catalytic site and a second distal site of the enzyme in agreement with the inhibitory behavior displayed by some recently reported²³ bis-tetrahydro-aminoacridine inhibitors of AChE.

The reversibility of action of **9** was assessed by dialysis in comparison to prototype **3** and tacrine. It was found that AChE activity blocked by tacrine was fully regenerated after 5 h, whereas following blockade by **9** only 50% of AChE activity could be reversed after 15 h and AChE inhibition could be detected also after 24 h (Figure 6). The longer duration of action displayed by **9** could tentatively be ascribed to a limited number and access of water molecules in the gorge, owing to the binding with a peripheral site besides the catalytic site of AChE.

In an attempt to rationalize the long duration of action of **9** (Figure 6), we computationally investigated the capability of both **9** and a reference AChE inhibitor (tacrine) to displace water molecules from the enzyme gorge. We took advantage of a purposely built AChE/**9** docking model and of the crystallographic structure of the AChE/tacrine complex.²⁴ Then, by means of the Insight II software²⁵ (default parameters were used), we obtained a rough estimate of the number of water molecules present in the AChE gorge both in the presence and in the absence of ligands.

The simulations with the inhibitors showed that while tacrine displaced only six water molecules, **9** was able

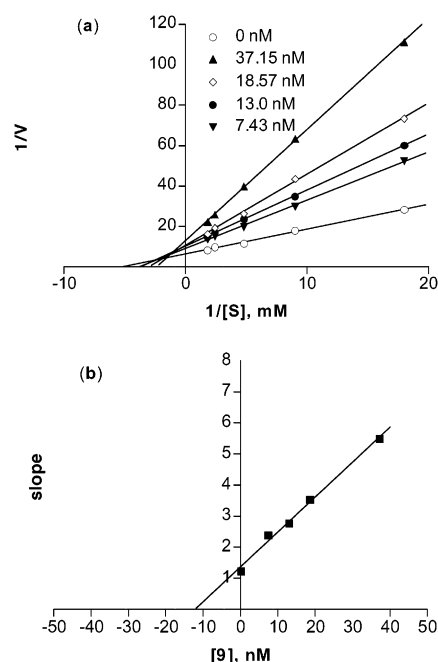


Figure 5. Steady-state inhibition by **9** of AChE hydrolysis of acetylthiocholine. Reciprocal plot of initial velocity and substrate concentration (a) and replot of the reciprocal plot versus inhibitor concentration (b) are reported. Reciprocal plot of initial velocity in the absence of inhibitor gave an estimate of k_{app} for acetylthiocholine of $170 \pm 15 \mu\text{M}$ (four experiments). Lines were derived from a weighted least-squares analysis of the data points.

Table 3. Inhibition Constants of AChE Obtained with **9** in Comparison with **3** and Tacrine^a

no.	AChE K_i (nM)
9	12.2 ± 0.6
3	104 ± 16
tacrine	151 ± 16

^a Inhibition constants, expressed as K_i values, were calculated from kinetic data in Figure 5.

to move from the AChE gorge as many as 16 water molecules (Figure 7). These numbers can be considered only as an indication of the number of water molecules involved in the formation of the AChE/ligand complex, and their absolute value can vary depending on such factors as the conformational state of the side chains of the residues lining the gorge or the computational scheme used to calculate them. However, the difference between **9** and tacrine is significant and reflects the different level of occupancy of the enzyme cavity by the two ligands.

Considering the much slower regeneration of the enzyme after inhibition by **9** compared to that after inhibition by tacrine (Figure 6), one might relate this phenomenon to the difficulty of resolating the gorge, that seems greater when a molecule such as **9** is present than when tacrine occupies the cavity. Actually, it is reasonable that, in the case of **9**, a larger number of water molecules have to find their way to penetrate into the gorge, than in the case of tacrine. Interestingly, recent crystallographic and theoretical studies on AChE reached the conclusion that the number of water molecules able to fill the enzyme gorge is about 20.^{26,27} Despite the approximation in the determination, the number of 16 referred to the water molecules displaced by **9** is consistent with a wide occupation of the AChE

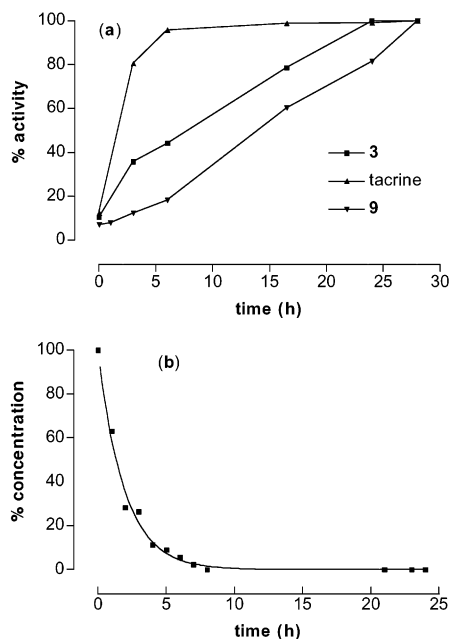


Figure 6. Time course of AChE regeneration after inhibition by 8.5, 0.85, and 13 μM concentration of **3**, **9**, and tacrine, respectively (a), and time course of elimination of **9** at 0.85 μM concentration from dialysis bag in the absence of AChE determined by HPLC (b).

gorge: as a consequence, it might be hypothesized that the process of enzyme regeneration is slowed because of the limited possibility of water molecules to diffuse in and of the inhibitor molecule to diffuse out the binding cavity.

Conclusions

We carried out an extensive SAR study of the potential anti-Alzheimer lead caproctamine (**3**), mainly with regard to the anti-cholinesterase activity. Variation of the alkyl group on the amine nitrogen of **3** led us to identify the ethyl group as the best substituent on that function, while the modification of the alkyl on the inner nitrogen atoms did not seem to affect significantly the activity. The substitutions introduced at the ortho position of the phenyl ring showed a clear effect on the inhibition of AChE related to the electronic influence of the substituents on the ionization of the nearby tertiary amine. After the evaluation of both AChE and BChE inhibitory potency, of the ability of reversing the D-tubocurarine-induced neuromuscular blockade, and of the antagonistic activity on muscarinic M_2 receptors, we individuated compound **9** as a promising derivative endowed of interesting biological characteristics making it worthy of further study in the field of Alzheimer therapeutics.

Experimental Section

Chemistry. Melting points were taken in glass capillary tubes on a Buechi SMP-20 apparatus and are uncorrected. IR, electron impact (EI) mass, and NMR spectra were recorded on Perkin-Elmer 297, VG 7070E, and Varian VXR 300 instruments, respectively. Chemical shifts are reported in parts per million (ppm) relative to tetramethylsilane (TMS), and spin multiplicities are given as s (singlet), br s (broad singlet), d (doublet), t (triplet), q (quartet), or m (multiplet). Although IR spectra data are not included (because of the lack of unusual features), they were obtained for all compounds reported and

were consistent with the assigned structures. The elemental compositions of the compounds agreed to within $\pm 0.4\%$ of the calculated value. When the elemental analysis is not included, crude compounds were used in the next step without further purification. Chromatographic separations were performed on silica gel columns by flash (Kieselgel 40, 0.040–0.063 mm; Merck), medium pressure (Biotage, KP–SIL 60, 0.032–0.063 mm), or gravity column (Kieselgel 60, 0.063–0.200 mm; Merck) chromatography. Reactions were followed by thin-layer chromatography (TLC) on Merck (0.25 mm) glass-packed precoated silica gel plates (60 F254) that were visualized in an iodine chamber. The term “dried” refers to the use of anhydrous sodium sulfate. Compounds were named following IUPAC rules as applied by Beilstein-Institut AutoNom (version 2.1), a PC integrated software package for systematic names in organic chemistry.

***N,N*-Diisopropyloctane-1,8-diamine (26).** A mixture of octane-1,8-diamine (0.72 g, 5 mmol), molecular sieves (3 Å), and acetone (1.1 mL, 15 mmol) in EtOH (20 mL) was stirred for 30 min at room temperature, and then an excess of NaBH_4 (0.9 g, 23.79 mmol) was added, and the stirring was continued for 6 h. Following removal of molecular sieves, the solution was made acidic with 6 N HCl. Removal of the solvent gave a residue that was dissolved in water (40 mL). The solution was washed with ether (3×20 mL) to remove nonbasic materials, then was made basic with 2 N NaOH, and finally was extracted with CH_2Cl_2 (3×30 mL). Evaporation of the dried solvent afforded a residue that was purified by flash chromatography. Elution with $\text{CH}_2\text{Cl}_2/\text{EtOAc}/\text{MeOH}/\text{aqueous } 28\% \text{ ammonia}$ (5:4:1:0.3) gave **26** as a pale yellow oil: 0.85 g (75% yield); $^1\text{H NMR}$ (CDCl_3) δ 0.90 (d, 12H), 1.12–1.38 (m, 12H + 2H exchangeable with D_2O), 2.43 (t, 4H), 2.63 (m, 2H); EI MS m/z 228 (M^+).

[5-({8-[(6-Benzyloxycarbonylamino)hexanoyl]isopropylamino}octyl)isopropylcarbamoyl]pentyl]carbamic Acid Benzyl Ester (27). Ethyl chloroformate (0.7 mL, 7.3 mmol) in dry dioxane (10 mL) was added dropwise to a stirred and cooled (5 °C) solution of *N*-[(benzyloxy)carbonyl]-6-aminocaproic acid (1.7 g, 6.4 mmol) and triethylamine (0.9 mL, 6.4 mmol) in dioxane (30 mL), followed after standing for 30 min by the addition of **26** (0.7 g, 3 mmol) in dioxane (20 mL). After the mixture was stirred at room temperature for 72 h, it was evaporated, affording a residue that was suspended in water (100 mL). The aqueous mixture was extracted with CHCl_3 (4×20 mL). The organic phase was washed with 2 N NaOH, 2 N HCl, and brine. Removal of the dried solvent gave a yellow oil that was purified by flash chromatography. Elution with $\text{CH}_2\text{Cl}_2/\text{EtOAc}/\text{EtOH}$ (8.7:1:0.3) afforded **27** as a pale yellow oil: 0.8 g (37% yield); $^1\text{H NMR}$ (CDCl_3) δ 1.05–1.66 (m, 36H), 2.20–2.32 (m, 4H), 2.99–3.21 (m, 8H), 3.92–4.05 (m, 1H), 4.56–4.68 (m, 1H), 4.78–4.86 (br s, 2H exchangeable with D_2O), 5.04 (s, 4H), 7.24–7.35 (m, 10H); EI MS m/z 723 (M^+).

6-Aminoheptanoic Acid {8-[(6-Amino)hexanoyl]isopropylamino}octyl}isopropylamide (28). A solution of 30% HBr in acetic acid (25 mL) was added to a solution of **27** (2.28 g, 3.1 mmol) in acetic acid and the resulting mixture was stirred for 4 h at room temperature. Ether (100 mL) was then added, yielding an oil, which was washed with ether (3×20 mL) and dissolved in water (50 mL). The solution was made basic with KOH pellets and extracted with CHCl_3 (3×30 mL). Removal of the dried solvent gave **28** in quantitative yield: $^1\text{H NMR}$ (CDCl_3) δ 1.05–1.61 (m, 36H), 2.11–2.29 (m, 4H), 2.38–2.51 (br s, 4H exchangeable with D_2O), 2.62 (t, 4H), 2.92–3.08 (m, 4H), 3.90–4.06 (m, 1H), 4.51–4.63 (m, 1H).

6-Isopropylaminoheptanoic Acid {8-[(6-Isopropylamino)hexanoyl]methylamino}octyl}methylamide (40). A solution of **29**¹⁴ (1.12 g, 2.8 mmol) in acetone (50 mL) was hydrogenated over 10% Pd on charcoal for 4 h. Following catalyst removal, the solvent was evaporated, obtaining a residue that was purified by flash chromatography. Elution with MeOH/aqueous 28% ammonia (9:1) afforded **40** as an oil: 30% yield; $^1\text{H NMR}$ (CDCl_3) δ 1.02 (d, 12H), 1.20–1.69 (m, 24H), 2.15–2.38 (m, 4H + 2H exchangeable with D_2O),

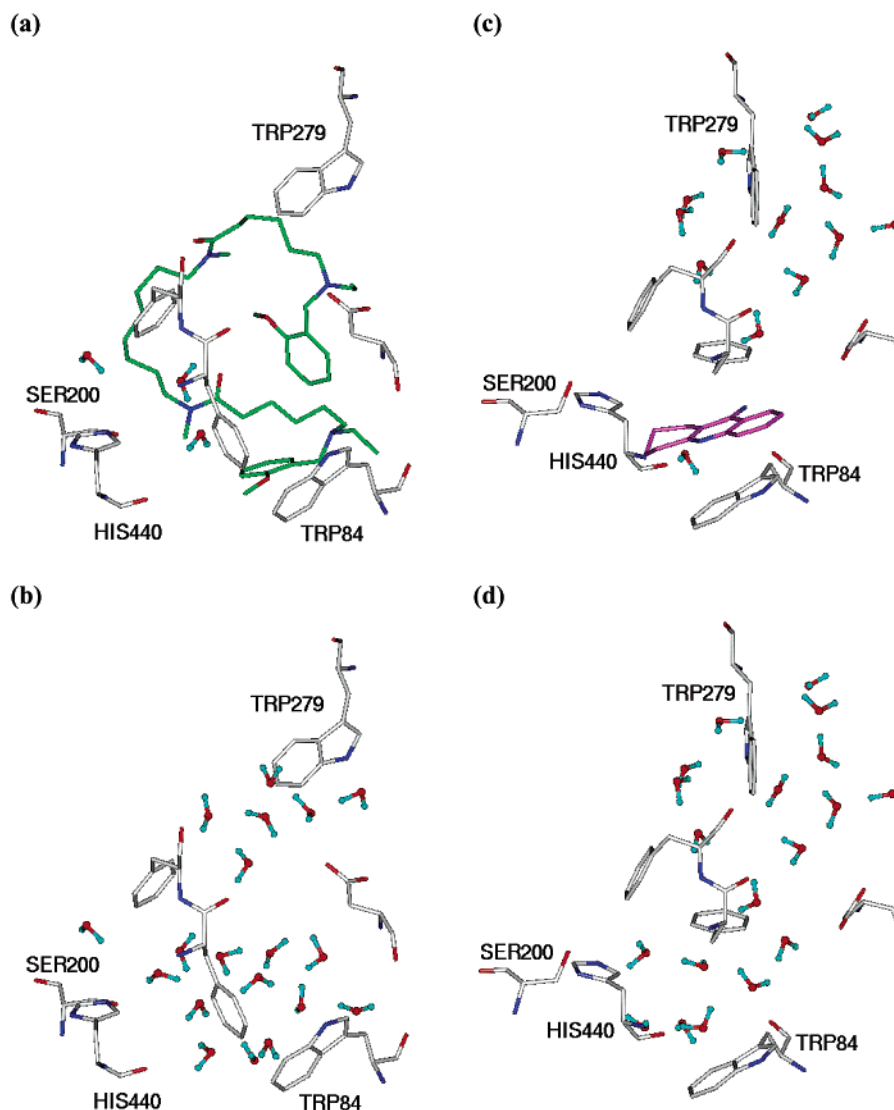


Figure 7. Docking model of the solvated **9**/AChE complex: three water molecules are present in the gorge (a). The solvated AChE gorge after the removal of **9**. The enzyme active site hosts 19 water molecules: 16 water molecules can be displaced by the interaction between **9** and AChE (b). Solvated tacrine/AChE docking complex (crystal structure): 13 water molecules are present in the gorge (c). The solvated tacrine/AChE docking complex after the removal of tacrine. The enzyme active site hosts 19 water molecules: six water molecules can be displaced by the interaction between tacrine and AChE (d). Water molecules are in ball-and-stick representation. The carbon atoms of **9** and tacrine are green and magenta, respectively.

2.57 (t, 4H), 2.66–2.86 (m, 2H) 2.90 (s, 3H), 2.98 (s, 3H), 3.16–3.38 (m, 4H); EI MS m/z 482 (M^+).

6-[Isopropyl-(2-methoxybenzyl)amino]hexanoic Acid [8-({6-[Isopropyl-(2-methoxybenzyl)amino]hexanoyl}-methylamino)octyl]methylamide Dioxalate (22). A mixture of **40** (0.18 g, 0.38 mmol) and 2-methoxybenzyl chloride (0.12 g, 0.76 mmol) in dry DMF (4 mL) was stirred for 36 h at room temperature. The removal of the solvent gave a residue that was purified by flash chromatography. Elution with $CH_2Cl_2/MeOH/aqueous$ 28% ammonia (10:0.5:0.05) afforded **22** as a pale yellow oil, which was transformed into the dioxalate salt: 25% yield; 1H NMR (free base, $CDCl_3$) δ 1.05 (d, 12H), 1.40–1.80 (m, 24H), 1.98–2.10 (m, 2H), 2.20–2.38 (m, 4H), 2.41–2.46 (m, 4H), 2.93 (d, 6H), 3.19–3.40 (m, 4H), 3.48–3.70 (m, 4H), 3.82 (s, 6H), 6.80–7.02 (m, 4H), 7.19–7.22 (m, 2H), 7.50–7.60 (m, 2H); EI MS m/z 723 (M^+). Anal. ($C_{48}H_{78}N_4O_{12}$) C, H, N.

General Procedure for the Synthesis of 6-Benzylaminohexanoic Acid {8-[(6-Benzylaminohexanoyl)methylamino]octyl}methylamide (30), 6-(2-Chlorobenzylamino)hexanoic Acid (8-[(6-(2-Chlorobenzylamino)hexanoyl)methylamino]octyl)methylamide (31), 6-(2-Trifluoromethylbenzylamino)hexanoic Acid Methyl-(8-{methyl-

[6-(2-trifluoromethylbenzylamino)hexanoyl]amino}octyl)amide (32), 6-(2-Propoxybenzylamino)hexanoic Acid Methyl-(8-{methyl-[6-(2-propoxybenzylamino)hexanoyl]amino}octyl)amide (34), 6-(2-Methylbenzylamino)hexanoic Acid Methyl-(8-{methyl-[6-(2-methylbenzylamino)hexanoyl]amino}octyl)amide (35), 6-(2-Nitrobenzylamino)hexanoic Acid Methyl-(8-{methyl-[6-(2-nitrobenzylamino)hexanoyl]amino}octyl)amide (36), 6-(3-Methoxybenzylamino)hexanoic Acid (8-[(6-(3-Methoxybenzylamino)hexanoyl)methylamino]octyl)methylamide (37), 6-(4-Methoxybenzylamino)hexanoic Acid (8-[(6-(4-Methoxybenzylamino)hexanoyl)methylamino]octyl)methylamide (38), 6-(2-Methoxybenzylamino)hexanoic Acid Isopropyl-(8-{isopropyl-[6-(2-methoxybenzylamino)hexanoyl]amino}octyl)amide (39). A mixture of **29**¹⁴ for compounds **30–38**, or **28** for compound **39** and the suitable substituted benzaldehyde (in a 1:2 molar ratio) in toluene (50 mL) was stirred at the refluxing temperature in a Dean Stark apparatus for 6 h. Following solvent removal, the residue was taken up in EtOH (30 mL) and $NaBH_4$ was added and the stirring was continued at room temperature for 6 h. The mixture was then made acidic with 3 N HCl, filtered, and evaporated. The residue was dissolved in water, and the

resulting solution was washed with ether, made basic with 2 N NaOH, and extracted with CHCl_3 . Removal of the dried solvent afforded the desired compound as a yellow oil in 34–98% yields.

30: 56% yield; $^1\text{H NMR}$ (CDCl_3) δ 1.18–1.72 (m, 24H + 2H exchangeable with D_2O), 2.20–2.46 (m, 4H), 2.62 (t, 4H), 2.88 (s, 3H), 2.98 (s, 3H), 3.17–3.36 (m, 4H), 3.77 (s, 4H), 7.21–7.31 (m, 10H).

31: 62% yield; $^1\text{H NMR}$ (CDCl_3) δ 1.22–1.79 (m, 24H + 2H exchangeable with D_2O), 2.22–2.38 (m, 4H), 2.64 (t, 4H), 2.80 (s, 3H), 2.84 (s, 3H), 3.20–3.28 (m, 2H), 3.30–3.40 (m, 2H), 3.89 (s, 4H), 7.18–7.28 (m, 4H), 7.31–7.42 (m, 4H).

32: 58% yield; $^1\text{H NMR}$ (CDCl_3) δ 1.17–1.64 (m, 24H + 2H exchangeable with D_2O), 2.22 (t, 4H), 2.55–2.62 (m, 4H), 2.80–2.85 (m, 6H), 3.13–3.31 (m, 4H), 3.85 (s, 4H), 7.21–7.30 (m, 2H), 7.40–7.59 (m, 6H).

34: 56% yield; $^1\text{H NMR}$ (CDCl_3) δ 0.99 (t, 6H), 1.10–1.82 (m, 28H + 2H exchangeable with D_2O), 2.11–2.28 (m, 4H), 2.53 (t, 4H), 2.83 (s, 3H), 2.87 (s, 3H), 3.10–3.32 (m, 4H), 3.73 (s, 4H), 3.87 (t, 4H), 6.72–6.88 (m, 4H), 7.09–7.25 (m, 4H).

35: 93% yield; $^1\text{H NMR}$ (CDCl_3) δ 1.11–1.60 (m, 24H + 2H exchangeable with D_2O), 2.15–2.25 (m, 10H), 2.57 (t, 4H), 2.79 (s, 3H), 2.82 (s, 3H), 3.16 (t, 2H), 3.21 (t, 2H), 3.64 (s, 4H), 7.00–7.27 (m, 8H).

36: 74% yield; $^1\text{H NMR}$ (CDCl_3) δ 1.18–1.79 (m, 24H + 2H exchangeable with D_2O), 2.26–2.32 (m, 4H), 2.50–2.62 (m, 4H), 2.85–2.98 (m, 6H), 3.18–3.38 (m, 4H), 3.98–4.01 (m, 4H), 7.24–7.92 (m, 8H).

37: 39% yield; $^1\text{H NMR}$ (CDCl_3) δ 1.15–1.74 (m, 24H + 2H exchangeable with D_2O), 2.15–2.40 (m, 4H), 2.51–2.74 (m, 4H), 2.79–3.02 (m, 6H), 3.07–3.43 (m, 4H), 3.59–3.97 (m, 10H), 6.67–7.00 (m, 6H), 7.07–7.33 (m, 2H); EI MS m/z 638 (M^+).

38: 38% yield; $^1\text{H NMR}$ (CDCl_3) δ 1.26–1.81 (m, 24H + 2H exchangeable with D_2O), 2.20–2.33 (m, 4H), 2.63 (t, 4H), 2.92 (d, 6H), 3.20–3.28 (m, 2H), 3.30–3.36 (m, 2H), 3.73 (s, 4H), 3.80 (s, 6H), 6.84–6.87 (d, 4H), 7.22–7.26 (d, 4H).

39: 34% yield; $^1\text{H NMR}$ (CDCl_3) δ 1.10–1.85 (m, 36H + 2H exchangeable with D_2O), 2.21–2.37 (m, 4H), 2.61 (t, 4H), 2.98–3.19 (m, 4H), 3.79 (s, 4H), 3.85 (s, 6H), 3.86–4.05 (m, 1H), 4.58–4.65 (m, 1H), 6.80–6.95 (m, 4H), 7.18–7.30 (m, 4H); EI MS m/z 695 (M^+).

6-[(3-Methoxybenzyl)methylamino]hexanoic Acid [8-((6-[(3-Methoxybenzyl)methylamino]hexanoyl)methylamino)octyl]methylamide Dioxalate (4) and 6-[(4-Methoxybenzyl)methylamino]hexanoic Acid [8-((6-[(4-Methoxybenzyl)methylamino]hexanoyl)methylamino)octyl]methylamide Dioxalate (5). A solution of **37** or **38** (0.21 mmol) in 95% HCOOH (0.5 mL) and 37% HCHO (0.5 mL) was refluxed for 12 h. The solution was made basic with 40% NaOH and extracted with CHCl_3 (3 \times 10 mL). Removal of the dried solvent gave a residue that was purified by flash chromatography. Elution with $\text{CHCl}_3/\text{MeOH}/\text{aqueous 28\% ammonia}$ (9:1:0.1) gave **4** or **5** that was converted into the dioxalate salt.

4: 95% yield; $^1\text{H NMR}$ (free base, CDCl_3) δ 1.19–1.67 (m, 24H), 2.16 (s, 6H), 2.20–2.38 (m, 8H), 2.88 (s, 3H), 2.93 (s, 3H), 3.18–3.36 (m, 4H), 3.42 (s, 4H), 3.78 (s, 6H), 6.70–6.89 (m, 6H), 7.11–7.25 (m, 2H); EI MS m/z 666 (M^+). Anal. ($\text{C}_{44}\text{H}_{70}\text{N}_4\text{O}_{12}$) C, H, N.

5: 81% yield; $^1\text{H NMR}$ (free base, CDCl_3) δ 1.25–1.73 (m, 24H), 2.15 (s, 6H), 2.20–2.37 (m, 8H), 2.90–2.94 (m, 6H), 3.16–3.40 (m, 8H), 3.79 (s, 6H), 6.81–6.86 (m, 4H), 7.18–7.21 (m, 4H); EI MS m/z 666 (M^+). Anal. ($\text{C}_{44}\text{H}_{70}\text{N}_4\text{O}_{12}$) C, H, N.

General Procedure for the Synthesis of Dioxalate Salts of 6-(Benzylethylamino)hexanoic Acid [8-((6-(Benzylethylamino)hexanoyl)methylamino)octyl]methylamide (6), 6-[(2-Chlorobenzyl)ethylamino]hexanoic Acid [8-((6-[(2-chlorobenzyl)ethylamino]hexanoyl)methylamino)octyl]methylamide (7), 6-[Ethyl-(2-trifluoromethylbenzyl)amino]hexanoic Acid [8-((6-[Ethyl-(2-trifluoromethylbenzyl)amino]hexanoyl)methylamino)octyl]methylamide (8), 6-[Ethyl-(2-methoxybenzyl)amino]hexanoic Acid [8-((6-[Ethyl-(2-methoxybenzyl)amino]hexanoyl)methylamino)octyl]methylamide (9), 6-[Ethyl-(2-propoxy-

benzyl)amino]hexanoic Acid [8-((6-[Ethyl-(2-propoxybenzyl)amino]hexanoyl)methylamino)octyl]methylamide (10), 6-[Ethyl-(2-methylbenzyl)amino]hexanoic Acid [8-((6-[Ethyl-(2-methylbenzyl)amino]hexanoyl)methylamino)octyl]methylamide (11), 6-[Ethyl-(2-nitrobenzyl)amino]hexanoic Acid [8-((6-[Ethyl-(2-nitrobenzyl)amino]hexanoyl)methylamino)octyl]methylamide (12), 6-[Ethyl-(2-methoxybenzyl)amino]hexanoic Acid [8-((6-[Ethyl-(2-methoxybenzyl)amino]hexanoyl)isopropylamino)octyl]isopropylamide (13), Ethyl-[6-(8-((6-[(6-ethyl-(2-methoxybenzyl)amino]hexyloxy)octyloxy)hexyl)-(2-methoxybenzyl)amine (23)). A mixture of **30**, **31**, **32**, **33**,¹⁰ **34**, **35**, **36**, **39**, or **41**¹⁵ and diethylsulfate (1:2.5 ratio) was refluxed for 48 h in toluene. Following removal of the solvent, the residue was taken up in water and made basic with KOH pellets and immediately extracted with CHCl_3 (3 \times 20 mL) or directly purified by column chromatography to avoid the quaternization of amine functions. Removal of the dried solvent gave a residue that was purified by flash chromatography. Elution with $\text{CH}_2\text{Cl}_2/\text{EtOAc}/\text{MeOH}/\text{aqueous 28\% ammonia}$ (5:4:1:0.1) gave the desired compound (**6–13**, or **23**) as a pale yellow oil in 20–82% yields, that was converted into the dioxalate salt (foam solid).

6: 20% yield; $^1\text{H NMR}$ (free base, CDCl_3) δ 1.00 (t, 6H), 1.24–1.68 (m, 24H), 2.24 (t, 4H), 2.38–2.52 (m, 8H), 2.88 (s, 3H), 2.94 (s, 3H), 3.18 (t, 2H), 3.28 (t, 2H), 3.53 (s, 4H), 7.16–7.31 (m, 10H); EI MS m/z 634 (M^+). Anal. ($\text{C}_{44}\text{H}_{70}\text{N}_4\text{O}_{10}$) C, H, N.

7: 58% yield; $^1\text{H NMR}$ (free base, CDCl_3) δ 0.97 (t, 6H), 1.12–1.68 (m, 24H), 2.20 (t, 4H), 2.38–2.48 (m, 8H), 2.81 (s, 3H), 2.86 (s, 3H), 3.14 (t, 2H), 3.24 (t, 2H), 3.56 (s, 4H), 7.05–7.19 (m, 4H), 7.21–7.25 (m, 2H), 7.43–7.46 (d, 2H); EI MS m/z 703 (M^+). Anal. ($\text{C}_{44}\text{H}_{68}\text{Cl}_2\text{N}_4\text{O}_{10}$) C, H, N.

8: 40% yield; $^1\text{H NMR}$ (free base, CDCl_3) δ 1.03 (t, 6H), 1.10–1.71 (m, 24H), 2.27 (t, 4H), 2.38–2.55 (m, 8H), 2.88 (s, 3H), 2.93 (s, 3H), 3.21 (t, 2H), 3.32 (t, 2H), 3.69 (s, 4H), 7.25 (t, 2H), 7.42–7.59 (m, 4H), 7.88 (d, 2H); EI MS m/z 770 (M^+). Anal. ($\text{C}_{46}\text{H}_{68}\text{F}_6\text{N}_4\text{O}_{10}$) C, H, N.

9: 58% yield; $^1\text{H NMR}$ (free base, CDCl_3) δ 1.12–1.72 (m, 30H), 2.28 (t, 4H), 2.59–2.79 (m, 8H), 2.90 (s, 3H), 2.96 (s, 3H), 3.19–3.38 (m, 4H), 3.82 (s, 10H), 6.82–6.98 (m, 4H), 7.21–7.32 (m, 2H), 7.48 (d, 2H); $^{13}\text{C NMR}$ (free base, CDCl_3) δ 173.11, 172.99, 157.93, 130.43, 128.48, 127.88, 120.54, 110.45, 55.61, 53.71, 51.53, 50.26, 50.20, 47.91, 35.58, 33.88 (N– CH_3), 33.60 (N– CH_3), 33.27 (N– CH_3), 29.96 and 29.67 and 29.59, 28.81, 27.77 and 27.68 and 27.51, 27.02, 25.74, 25.35, 11.96; EI MS m/z 695 (M^+). Anal. ($\text{C}_{46}\text{H}_{74}\text{N}_4\text{O}_{12}$) C, H, N.

10: 23% yield; $^1\text{H NMR}$ (free base, CDCl_3) δ 1.04 (t, 12H), 1.10–1.70 (m, 24H), 1.82 (q, 4H), 2.25 (t, 4H), 2.42–2.59 (m, 8H), 2.89 (s, 3H), 2.94 (s, 3H), 3.21 (t, 2H), 3.32 (t, 2H), 3.61 (s, 4H), 3.92 (t, 4H), 6.80–6.95 (m, 4H), 7.18 (t, 2H), 7.42 (d, 2H); EI MS m/z 751 (M^+). Anal. ($\text{C}_{50}\text{H}_{82}\text{N}_4\text{O}_{12}$) C, H, N.

11: 82% yield; $^1\text{H NMR}$ (free base, CDCl_3) δ 1.01 (t, 6H), 1.12–1.72 (m, 24H), 2.20–2.55 (m, 18H), 2.89 (s, 3H), 2.93 (s, 3H), 3.21 (t, 2H), 3.32 (t, 2H), 3.48 (s, 4H), 7.10–7.38 (m, 8H); EI MS m/z 663 (M^+). Anal. ($\text{C}_{46}\text{H}_{74}\text{N}_4\text{O}_{10}$) C, H, N.

12: 45% yield; $^1\text{H NMR}$ (free base, CDCl_3) δ 0.92 (t, 6H), 1.22–1.62 (m, 24H), 2.20–2.45 (m, 12H), 2.83 (s, 3H), 2.92 (s, 3H), 3.15–3.32 (m, 4H), 3.79 (s, 4H), 7.22–7.78 (m, 8H); EI MS m/z 725 (M^+). Anal. ($\text{C}_{44}\text{H}_{68}\text{N}_6\text{O}_{14}$) C, H, N.

13: 34% yield; $^1\text{H NMR}$ (free base, CDCl_3) δ 1.02–1.70 (m, 42H), 2.21–2.38 (q, 4H), 2.42–2.62 (m, 8H), 3.05–3.19 (q, 4H), 3.61 (s, 4H), 3.83 (s, 6H), 3.96–4.11 (m, 1H), 4.61–4.75 (m, 1H), 6.81–6.99 (m, 4H), 7.18–7.33 (m, 2H), 7.45 (d, 2H); EI MS m/z 751 (M^+). Anal. ($\text{C}_{50}\text{H}_{82}\text{N}_4\text{O}_{12}$) C, H, N.

23: 20% yield; $^1\text{H NMR}$ (free base, CDCl_3) δ 1.04 (t, 6H), 1.25–1.62 (m, 28H), 2.44 (t, 4H), 2.51 (q, 4H), 3.37 (t, 8H), 3.58 (s, 4H), 3.81 (s, 6H), 6.83 (d, 2H), 6.88 (t, 2H), 7.19–7.42 (t, 2H), 7.40 (d, 2H); EI MS m/z 640 (M^+). Anal. ($\text{C}_{44}\text{H}_{72}\text{N}_2\text{O}_{12}$) C, H, N.

General Procedures for the Synthesis of Methiodides 14–21 and 24. A solution of the appropriate compound (**6–13** or **23**) as the free base in acetone (15 mL) was treated with methyl iodide (1:10 molar ratio). After standing overnight at

room temperature, the solvent was removed and the residue was triturated with ether to give a foam pale yellow solid in quantitative yield.

14: $^1\text{H NMR}$ (DMSO- d_6) δ 1.01–1.77 (m, 30H), 2.18–2.31 (m, 4H), 2.71 (s, 3H), 2.78 (s, 6H), 2.86 (s, 3H), 3.00–3.25 (m, 12H), 4.40 (s, 4H), 7.47 (s, 10H). Anal. ($\text{C}_{42}\text{H}_{72}\text{I}_2\text{N}_4\text{O}_2$) C, H, N.

15: $^1\text{H NMR}$ (DMSO- d_6) δ 1.04 (t, 6H), 1.21–1.77 (m, 24H), 2.28 (m, 4H), 2.76 (s, 3H), 2.90 (s, 9H), 3.01–3.35 (m, 12H), 4.61 (s, 4H), 7.49–7.68 (m, 8H). Anal. ($\text{C}_{42}\text{H}_{70}\text{Cl}_2\text{I}_2\text{N}_4\text{O}_2$) C, H, N.

16: $^1\text{H NMR}$ (DMSO- d_6) δ 1.15–1.78 (m, 30H), 2.23–2.31 (m, 4H), 2.74–2.92 (m, 12H), 3.15–3.51 (m, 12H), 4.69 (s, 4H), 7.76–7.98 (m, 8H). Anal. ($\text{C}_{44}\text{H}_{70}\text{F}_6\text{I}_2\text{N}_4\text{O}_2$) C, H, N.

17: $^1\text{H NMR}$ (DMSO- d_6) δ 1.26–1.75 (m, 30H), 2.12–2.19 (m, 4H), 2.77 (s, 3H), 2.82 (s, 6H), 2.91 (s, 3H), 3.06–3.56 (m, 12H), 3.84 (s, 6H), 4.43 (s, 4H), 7.03–7.21 (m, 4H), 7.41–7.59 (m, 4H). Anal. ($\text{C}_{44}\text{H}_{76}\text{I}_2\text{N}_4\text{O}_4$) C, H, N.

18: $^1\text{H NMR}$ (DMSO- d_6) δ 0.98 (t, 6H), 1.05–1.80 (m, 34H), 2.22–2.30 (m, 4H), 2.72 (s, 3H), 2.82 (s, 6H), 2.91 (s, 3H), 3.05–3.19 (m, 12H), 4.00 (t, 4H), 4.42 (s, 4H), 7.00–7.15 (m, 4H), 7.44–7.51 (m, 4H). Anal. ($\text{C}_{48}\text{H}_{84}\text{I}_2\text{N}_4\text{O}_4$) C, H, N.

19: $^1\text{H NMR}$ (DMSO- d_6) δ 1.10–1.92 (m, 30H), 2.25–2.34 (m, 4H), 2.48 (s, 6H), 2.84 (s, 3H), 2.94 (s, 3H), 3.07 (s, 6H), 3.18–3.76 (m, 12H), 4.77 (s, 4H), 7.21–7.34 (m, 6H), 7.51–7.59 (m, 2H). Anal. ($\text{C}_{44}\text{H}_{76}\text{I}_2\text{N}_4\text{O}_2$) C, H, N.

20: $^1\text{H NMR}$ (DMSO- d_6) δ 1.12–1.75 (m, 30H), 2.19–2.23 (m, 4H), 2.64–2.84 (m, 12H), 3.02–3.38 (m, 12H), 4.79 (s, 4H), 7.71–7.81 (m, 6H), 8.02–8.11 (m, 2H). Anal. ($\text{C}_{42}\text{H}_{70}\text{I}_2\text{N}_6\text{O}_6$) C, H, N.

21: $^1\text{H NMR}$ (DMSO- d_6) δ 1.03 (d, 6H), 1.08 (d, 6H), 1.23–1.79 (m, 30H), 2.19–2.31 (m, 4H), 2.79 (s, 6H), 2.92–3.31 (m, 12H), 3.82 (s, 6H), 3.96–4.06 (m, 2H), 4.40 (s, 4H), 7.03–7.16 (m, 4H), 7.40–7.50 (m, 4H). Anal. ($\text{C}_{48}\text{H}_{84}\text{I}_2\text{N}_4\text{O}_4$) C, H, N.

24: $^1\text{H NMR}$ (DMSO- d_6) δ 1.19–1.81 (m, 34H), 2.81 (s, 6H), 3.02–3.37 (m, 16H), 3.85 (s, 6H), 4.43 (s, 4H), 7.00–7.21 (m, 4H), 7.40–7.62 (m, 4H). Anal. ($\text{C}_{42}\text{H}_{74}\text{I}_2\text{N}_2\text{O}_4$) C, H, N.

Biology. Functional Antagonism. Male guinea pigs (200–300 g) and male Wistar rats (280–300 g) were killed by cervical dislocation. The organs required were set up rapidly under 1 g of tension in 20 mL organ baths containing physiological salt solution (PSS) maintained at an appropriate temperature and aerated with 5% CO_2 –95% O_2 .

Guinea Pig Left Atria. The heart was rapidly removed, and right and left atria were separated out. The left atria were mounted at 30 °C in PSS of the following composition (mM): NaCl, 118; KCl, 4.7; CaCl_2 , 2.52; $\text{MgSO}_4 \cdot 7\text{H}_2\text{O}$, 1.18; KH_2PO_4 , 1.18; NaHCO_3 , 23.8; glucose, 11.7. Tissues were stimulated through platinum electrodes by square-wave pulses (1 ms, 1 Hz, 5–10 V) (Tetra Stimulus, N. Zagoni). Inotropic activity was recorded isometrically. Tissues were equilibrated for 2 h and a cumulative concentration–response curve to APE was constructed. Concentration–response curves were constructed by cumulative addition of the reference agonist. The concentration of agonist in the organ bath was increased approximately 3-fold at each step, with each addition being made only after the response to the previous addition had attained a maximal level and remained steady. Following 30 min of washing, tissues were incubated with the antagonist for 1 h, and a new dose–response curve to the agonist was obtained. Contractions were recorded by means of a force displacement transducer connected to the MacLab system PowerLab/800. In addition parallel experiments in which tissues did not receive any antagonist were run to check any variation in sensitivity.

To quantify antagonist potency, pK_b values were calculated from the equation $pK_b = \log(\text{DR} - 1) - \log[\text{B}]$, where DR is the ratio of EC_{50} values of agonist after and before treatment with 10 μM concentration of the antagonist $[\text{B}]$.²⁰

Rat Nerve-Hemidiaphragms. Right and left phrenic nerve-hemidiaphragms were used following a described procedure.^{17,18} Briefly, each phrenic nerve-hemidiaphragm was suspended at 25 °C in PSS of the following composition (mM): NaCl, 118; KCl, 4.8; CaCl_2 , 2.5; KH_2PO_4 , 1.2; $\text{MgSO}_4 \cdot 7\text{H}_2\text{O}$,

1.2; NaHCO_3 , 25; glucose, 11.1. Effects of AChE inhibitors on neuromuscular junction were assessed as the ability of reversing the partial blockade induced by D-tubocurarine in indirectly elicited twitch responses. Twitches were obtained by stimulating the phrenic nerve with square pulses of 0.5-ms duration at 0.2 Hz and supramaximal voltage. Neuromuscular blockade was obtained with the addition of D-tubocurarine (1–5 μM). Drugs were added when a reduction of the twitch response of 70–80% of control values was obtained. The effect of each drug was evaluated after 15 min of exposure. To avoid the possible carry-over effects, only one concentration of inhibitor was tested on each preparation. Several drug concentrations were evaluated for each AChE inhibitor. To quantify the reversal effect of each drug, the antagonism index (AI or percent of antagonism)¹⁷ was determined for each concentration and the AI_{50} (drug concentration that gives a 50% value of AI) was calculated.

Inhibition of AChE and BChE. The method of Ellman et al. was followed.¹⁶ Five different concentrations of each compound were used to obtain inhibition of AChE or BChE activity comprised between 20 and 80%. The assay solution consisted of a 0.1 M phosphate buffer pH 8.0, with the addition of 340 μM 5,5'-dithio-bis(2-nitrobenzoic acid), 0.035 unit/mL AChE or BChE derived from human erythrocytes (0.39 and 5.9 UI/mg, respectively; Sigma Chemical), and 550 μM acetylthiocholine iodide. Test compounds were added to the assay solution and preincubated at 37 °C with the enzyme for 20 min followed by the addition of substrate. Assays were done with a blank containing all components except AChE or BChE to account for nonenzymatic reaction. The reaction rates were compared and the percent inhibition due to the presence of test compounds was calculated. Each concentration was analyzed in triplicate, and IC_{50} values were determined graphically from log concentration–inhibition curves.

To ascertain the effect of pH on the inhibition of AChE activity, experiments were also carried out at pH values of 7.0 and 7.5 for few selected inhibitors.

Determination of Steady-State Inhibition Constant. To obtain estimates of the competitive inhibition constant K_i , reciprocal plots of $1/V$ versus $1/[\text{S}]$ were constructed at relatively low concentration of substrate (below 0.5 mM). The plots were assessed by a weighted least-squares analysis that assumed the variance of V to be a constant percentage of V for the entire data set. Slopes of these reciprocal plots were then plotted against $\mathbf{9}$ concentration (range 7–37 nM) in a similar weighted analysis and K_i was determined as the ratio of the replot intercept to the replot slope.

Reciprocal plots involving $\mathbf{9}$ inhibition show both increasing slopes (decreased V_{max} at increasing inhibitor's concentrations) and increasing intercepts (higher K_m) with higher inhibitor concentration. This pattern indicates mixed inhibition, arising from significant inhibitor interaction with both the free enzyme and the acetylated enzyme. Replots of the slope versus the concentration of $\mathbf{9}$ gives an estimate of competitive inhibition constant, $K_i = 12.2 \pm 0.6$ nM.

So the pattern in the graphical representation shows $\mathbf{9}$ able to bind to the peripheral anionic site as well as the active site.

Dialysis. Stock solutions in replicates were prepared as following: the free enzyme (0.39 units in 3 mL of 0.1 M phosphate buffer pH 8.0), the same amount of enzyme plus tacrine 13.0 μM , 8.5 μM **3**, and 0.85 μM **9**. The enzyme concentration was 10-fold higher than that used in the Ellman test, while the inhibitors' concentration was 50-fold higher than that of their IC_{50} values.

The solutions were gently stirred and incubated at 37 °C for 20 min. They were then loaded into 12,000 MW cutoff dialysis bags and dialyzed at 22 °C against 2 L of 0.1 M phosphate buffer pH 8.0. Dialysis was interrupted at fixed times up to 30 h. The solutions were five times diluted with the same buffer and kept at 20–22 °C under magnetic stirring. Aliquots of 0.95 mL of each solution were sampled and the enzyme activity spectrophotometrically tested after addition of 0.034 mL of DTNB and 0.016 mL of acetylthiocholine as described above. Plots of enzyme activities for each compound,

expressed as a percentage of the dialyzed free enzyme activity against time of dialysis, were calculated for each inhibitor. A HPLC method was used to monitor over the time the concentration of **9** incubated alone in the dialysis bag. The stationary phase was a 5 μm Phenyl-hexyl Luna Phenomenex (150 \times 3.0 mm i.d.) column, the mobile phase consisted of a mixture of acetonitrile/0.02 M triethylammonium phosphate (pH 4.0) (37:63 v/v), the flow rate was 0.4 mL min^{-1} and the UV detection was fixed at 220 nm. Compound **9** at 0.85 μM concentration in the dialysis bag, without enzyme, decreased to zero in 8 h.

Molecular Dynamics (MD) Simulations. An AChE/**9** docking model was built by taking advantage of the energetically relaxed complex between AChE and **3**.¹⁰ **9** was simply built by properly modifying **3**. With the aim of obtaining an energetically relaxed AChE/**9** docking model, MD simulations were carried out by using the united atom AMBER* force field as implemented in MacroModel Ver. 5.5.²⁸ Polar and aromatic hydrogen atoms were added to the protein, while the aliphatic portions were treated using the united atom model of AMBER.²⁹ It should be remarked that the aromatic ring modeling by means of the all atom model allowed properly accounting for the π -cation interaction,³⁰ fundamental when studying AChE/inhibitor complexes.³¹

Around the inhibitor (10 Å), a set of atoms was defined, which was allowed to freely move during the simulations. A shell was defined 3 Å around such a core of atoms. The atoms belonging to this shell were constrained by applying an energy penalty force constant of 100 kJ/mol Å⁻². Atoms beyond this shell were maintained at their crystallographic positions. This protocol has already been applied to relax AChE/inhibitor complexes.^{10,32,33}

On this system, a total of 300 ps of MD simulations were carried out and the last snapshot was energy minimized by both steepest descent and conjugate gradient until a convergence of 0.05 kJ/mol Å⁻¹ on the gradient was reached. This energy-minimized structure was then used for the subsequent solvation study.

Solvation Simulations. To study the water molecule displacement caused by both **9** and tacrine, some simulations were carried out by means of the software package Insight II.²⁵ First, the crystal structure of AChE/tacrine complex (PDB code: 1ACJ) and the energy minimized docking model of AChE/**9** were solvated. Then, the two inhibitors were removed from the gorge, and the protein was solvated again. This allowed us to detect the water molecules displaced by either tacrine or **9**. The procedure was repeated several times, and average numbers of displaced water molecules were obtained for **9** and tacrine, respectively.

Statistical Analysis. Data were analyzed using a pharmacological computer program.³⁴ Values are given as mean \pm standard error of n independent observations. Student's t -test was used to assess the statistical significance of the difference between two means.

Acknowledgment. This research was supported by Grants from the University of Bologna (Funds for Selected Research Topics) and MIUR.

References

- Bartus, R. T.; Dean, R. L., 3rd; Beer, B.; Lippa, A. S. The cholinergic hypothesis of geriatric memory dysfunction. *Science* **1982**, *217*, 408–414.
- Coyle, J. T.; Price, D. L.; DeLong, M. R. Alzheimer's disease: a disorder of cortical cholinergic innervation. *Science* **1983**, *219*, 1184–1190.
- Giacobini, E. Cholinesterase inhibitors: from the Calabar bean to Alzheimer therapy. *Cholinesterases and Cholinesterase Inhibitors*; Martin Dunitz Ltd: London, UK, 2000; pp 181–226.
- Kasa, P.; Rakonczay, Z.; Gulya, K. The cholinergic system in Alzheimer's disease. *Prog. Neurobiol.* **1997**, *52*, 511–535.
- Gualtieri, F.; Dei, S.; Manetti, D.; Romanelli, M. N.; Scapechi, S.; Teodori, E. The medicinal chemistry of Alzheimer's and Alzheimer-like diseases with emphasis on the cholinergic hypothesis. *Farmaco* **1995**, *50*, 489–503.
- Brufani, M.; Filocamo, L.; Lappa, S.; Maggi, A. New acetylcholinesterase inhibitors. *Drugs Future* **1997**, *22*, 397–410.
- Barril, X.; Orozco, M.; Luque, F. J. Towards improved acetylcholinesterase inhibitors: a structural and computational approach. *Mini Rev. Med. Chem.* **2001**, *1*, 255–266.
- Castro, A.; Martinez, A. Peripheral and dual binding site acetylcholinesterase inhibitors: implications in treatment of Alzheimer's disease. *Mini Rev. Med. Chem.* **2001**, *1*, 267–272.
- Inestrosa, N. C.; Alvarez, A.; Perez, C. A.; Moreno, R. D.; Vicente, M.; Linker, C.; Casanueva, O. I.; Soto, C.; Garrido, J. Acetylcholinesterase accelerates assembly of amyloid-beta-peptides into Alzheimer's fibrils: possible role of the peripheral site of the enzyme. *Neuron* **1996**, *16*, 881–891.
- Part I: Melchiorre, C.; Andrisano, V.; Bolognesi, M. L.; Budriesi, R.; Cavalli, A.; Cavrini, V.; Rosini, M.; Tumiatti, V.; Recanatini, M. Acetylcholinesterase noncovalent inhibitors based on a polyamine backbone for potential use against Alzheimer's disease. *J. Med. Chem.* **1998**, *41*, 4186–4189.
- Melchiorre, C.; Yong, M. S.; Benfey, B. G.; Belleau, B. Molecular properties of the adrenergic α -receptor. 2. Optimum covalent inhibition by two different prototypes of polyamine disulfides. *J. Med. Chem.* **1978**, *21*, 1126–1132.
- Benfey, B. G.; Yong, M. S.; Belleau, B.; Melchiorre, C. Cardiac muscarinic blocking and atropinic blocking effects of a tetramine disulfide and α -adrenoceptor blocking activity. *Can. J. Physiol. Pharmacol.* **1979**, *57*, 41–47.
- Benfey, B. G.; Brasili, L.; Melchiorre, C.; Belleau, B. Potentiation and inhibition of nicotinic effects on striated muscle by the tetramine disulfide benextramine. *Can. J. Physiol. Pharmacol.* **1980**, *58*, 984–988.
- Melchiorre, C.; Quaglia, W.; Picchio, M. T.; Giardinà, D.; Brasili, L.; Angeli, P. Structure–activity relationships among methoctramine-related polymethylene tetraamines. Chain-length and substituent effects on M₂ muscarinic receptor blocking activity. *J. Med. Chem.* **1989**, *32*, 79–84.
- Quaglia, W.; Giardinà, D.; Marucci, G.; Melchiorre, C.; Minarini, A.; Tumiatti, V. Structure–activity relationships among methoctramine-related polymethylene tetraamines. 3. Effect of the four nitrogens on M₂ muscarinic blocking activity as revealed by symmetrical and unsymmetrical polyamines. *Farmaco* **1991**, *46*, 417–434.
- Ellman, G. L.; Courtney, K. D.; Andres, V.; Featherstone, R. M. A new rapid colorimetric determination of acetylcholinesterase activity. *Biochem. Pharmacol.* **1961**, *7*, 88–95.
- Riesz, M.; Kapati, E.; Szporny, L. Antagonism of non-depolarising neuromuscular blockade by aminopyridines in cats. *J. Pharm. Pharmacol.* **1986**, *38*, 156–158.
- Bosch, F.; Morales, M.; Badia, A.; Banos, J. E. Comparative effects of velnacrine, tacrine and physostigmine on the twitch responses in the rat phrenic-hemidiaphragm preparation. *Gen. Pharmacol.* **1993**, *24*, 1101–1105.
- Minarini, A.; Bolognesi, M. L.; Budriesi, R.; Canossa, M.; Chiarini, A.; Spampinato, S.; Melchiorre, C. Design, synthesis, and biological activity of methoctramine-related tetraamines bearing an 11-acetyl-5, 11-dihydro-6H-pyrido[2,3-b][1,4]benzodiazepin-6-one moiety: structural requirements for optimum occupancy of muscarinic receptor subtypes as revealed by symmetrical and unsymmetrical polyamines. *J. Med. Chem.* **1994**, *37*, 3363–3372.
- Van Rossum, J. M. Cumulative dose–response curves. II. Technique for the making of dose–response curves in isolated organs and the evaluation of drug parameters. *Arch. Int. Pharmacodyn. Ther.* **1963**, *143*, 299–330.
- Bartolini, M.; Bertucci, C.; Gotti, R.; Tumiatti, V.; Cavalli, A.; Recanatini, M.; Andrisano, V. Determination of the dissociation constants (pK_a) of basic acetylcholinesterase inhibitors by reversed-phase liquid chromatography. *J. Chromatogr. A* **2002**, *958*, 59–67.
- Camps, P.; El Achab, R.; Gorbic, D. M.; Morral, J.; Munoz-Torrero, D.; Badia, A.; Eladi Banos, J.; Vivas, N. M.; Barril, X.; Orozco, M.; Luque, F. J. Synthesis, in vitro pharmacology, and molecular modeling of very potent tacrine-huperzine A hybrids as acetylcholinesterase inhibitors of potential interest for the treatment of Alzheimer's disease. *J. Med. Chem.* **1999**, *42*, 3227–3242.
- Pang, Y. P.; Quiram, P.; Jelacic, T.; Hong, F.; Brimijoin, S. Highly potent, selective, and low cost bis-tetrahydroaminacrine inhibitors of acetylcholinesterase. Steps toward novel drugs for treating Alzheimer's disease. *J. Biol. Chem.* **1996**, *271*, 23646–23649.
- Sussman, J. L.; Harel, M.; Silman, I. Three-dimensional structure of acetylcholinesterase and of its complexes with anticholinesterase drugs. *Chem. Biol. Interact.* **1993**, *87*, 187–197.
- Insight II*; 98.0 ed.; MSI: San Diego.
- Koellner, G.; Kryger, G.; Millard, C. B.; Silman, I.; Sussman, J. L.; Steiner, T. Active-site gorge and buried water molecules in crystal structures of acetylcholinesterase from *Torpedo californica*. *J. Mol. Biol.* **2000**, *296*, 713–735.
- Henchman, R. H.; Tai, K.; Shen, T.; McCammon, J. A. Properties of water molecules in the active site gorge of acetylcholinesterase from computer simulation. *Biophys. J.* **2002**, *82*, 2671–2682.

- (28) Mohamadi, F.; Richards, N. G. J.; Guida, W. C.; Liskamp, R. M. J.; Lipton, M. A.; Caulfield, C. E.; Chang, G.; Hendrickson, T. F.; Still, W. C. MacroModel – An integrated software system for modeling organic and bioorganic molecules using molecular mechanics. *J. Comput. Chem.* **1990**, *1*, 440–467.
- (29) Weiner, S. J.; Kollman, P. A.; Case, D. A.; Singh, U. C.; Ghio, C.; Alagona, G.; Profeta, S.; Weiner, P. A new force field for molecular mechanical simulation of nucleic acids and proteins. *J. Am. Chem. Soc.* **1984**, *106*, 765–784.
- (30) Dougherty, D. A. Cation- π interactions in chemistry and biology: a new view of benzene, Phe, Tyr, and Trp. *Science* **1996**, *271*, 163–168.
- (31) Pang, Y. P.; Kozikowski, A. P. Prediction of the binding site of 1-benzyl-4-[(5,6-dimethoxy-1-indanon-2-yl)methyl]piperidine in acetylcholinesterase by docking studies with the SYSDOC program. *J. Comput. Aided Mol. Des.* **1994**, *8*, 683–693.
- (32) Rampa, A.; Bisi, A.; Valenti, P.; Recanatini, M.; Cavalli, A.; Andrisano, V.; Cavrini, V.; Fin, L.; Buriani, A.; Giusti, P. Acetylcholinesterase inhibitors: synthesis and structure–activity relationships of omega-[N-methyl-N-(3-alkylcarbamoyloxy-phenyl)-methyl]aminoalkoxyheteroaryl derivatives. *J. Med. Chem.* **1998**, *41*, 3976–3986.
- (33) Andreani, A.; Cavalli, A.; Granaiola, M.; Guardigli, M.; Leoni, A.; Locatelli, A.; Morigi, R.; Rambaldi, M.; Recanatini, M.; Roda, A. Synthesis and screening for antiacetylcholinesterase activity of (1-benzyl-4-oxopiperidin-3-ylidene)methylindoles and -pyrroles related to donepezil. *J. Med. Chem.* **2001**, *44*, 4011–4014.
- (34) Motulsky, H. J. *Analyzing Data with GraphPad Prism*; Graph-Pad Software Inc.: San Diego, CA, 1999.

JM021055+